ChemComm

# An unprecedented 2D covalent organic framework with an htb net topology



| | |
|---|---|
| Journal: | *ChemComm* |
| Manuscript ID | CC-COM-08-2019-006780.R1 |
| Article Type: | Communication |
| | |

Journal Name

COMMUNICATION

# An unprecedented 2D covalent organic framework with an htb net topology†

Received 00th January 20xx,
Accepted 00th January 20xx

DOI: 10.1039/x0xx00000x

www.rsc.org/

Song-Liang Cai,[a,b] Zi-Hao He,[a] Xin-Le Li,[b] Kai Zhang,[a] Sheng-Run Zheng,*[a] Jun Fan,[a] Yi Liu*[b] and Wei-Guang Zhang*[a]

**A 2D imine-linked COF with a hitherto unreported htb type topology was synthezied from a linear diamine linker and a judiciously designed tetra-aldehyde building block. This work opens the door to the development of COFs with unprecedented topologies and may broaden the scope of COF functional materials by pore size and pore surface engineering.**

Covalent organic frameworks (COFs), which are crystalline porous organic polymers with precise integration of building blocks into periodic two- or three-dimensional (2D or 3D) structures, have attracted significant attention due not only to their intriguing architectures and topologies,[1-7] but also to their various promising applications in heterogeneous catalysis,[8,9] gas storage,[10-12] chemical sensing,[13-15] chromatographic separation,[16-18] photoelectric device,[19-21] among others. Through extensive investigations over the past decade, a great number of COFs with interesting properties have been rationally designed and successfully constructed. Nevertheless, when compared to their counterparts, metal organic frameworks (MOFs),[22] the structural topologies of COFs are still extremely limited. This topology scarcity is attributable to the difference in coordination/bonding geometry of the building blocks: the topologies of MOFs can be varied by not only the structure of multidentate building blocks, but also the flexible coordination geometries of metal ions or clusters, while the topologies of COFs are mainly dependent on the geometry of organic building blocks used in the polymerization reactions, which represents a much smaller subset due to considerations on rigidity and symmetry.[1-3]

Owing to the limitation of available organic building blocks having particular configurations,[2] up to now, only six main types of structural topologies have been realized in the construction of 2D COF structures: **hcb**,[23] **sql**,[24] **hxl**,[25] **kgm**[26], **kgd**[27] and **tth**[28] nets. Recently, by employing a desymmetrized-vertex strategy,[29] or a mixed-linker or mixed-vertex strategy,[30-32] more complicated 2D COFs containing two or three different kinds of pores have been successfully constructed. However, from a topological perspective, all of these reported dual-pore and triple-pore 2D COFs can be simplified as one of the above-mentioned six nets. Consequently, the rational design of versatile molecular building blocks that enable the construction of 2D COFs with novel topologies is highly desired.

When designing 2D COFs with new topologies, much attention has been given to desymmetrized rigid linkers with pre-defined vertex angles. As these linkers are interconnected, a final topology is realized as a tessellated plane of mathematically tiled polygons.[1] Herein, we present the rational design, targeted construction and structural characterization of a novel 2D imine-based COF structure, namely BITA-PDA COF (Scheme **1**), by using a benzimidazole-based tetra-aldehyde (BITA) and phenylenediamine (PDA) as the monomers. The judiciously designed BITA building block is unique in that it functions as a 4-connected node with four specific angles between neighboring edges of benzaldehyde groups being ~60, 90, 90 and 120°, respectively, thus satisfying the geometrical requirement for the tessellation of a 3.4.6.4 Archimedean tiling

**Scheme 1** (a) The molecular structure of the tetra-aldehyde precursor **BITA** and the diamine linker **PDA**, and the resulting BITA-PDA 2D COF in an **htb** net topology. The chemically nonequivalent CHO groups are colored differently to underline their different reactivities. (b) A subunit of the COF structure highlighting the four-connected node with pre-defined vertex angles for the assembly of a 3.4.6.4 Archimedean tiling (equivalent to the **htb** net topology).

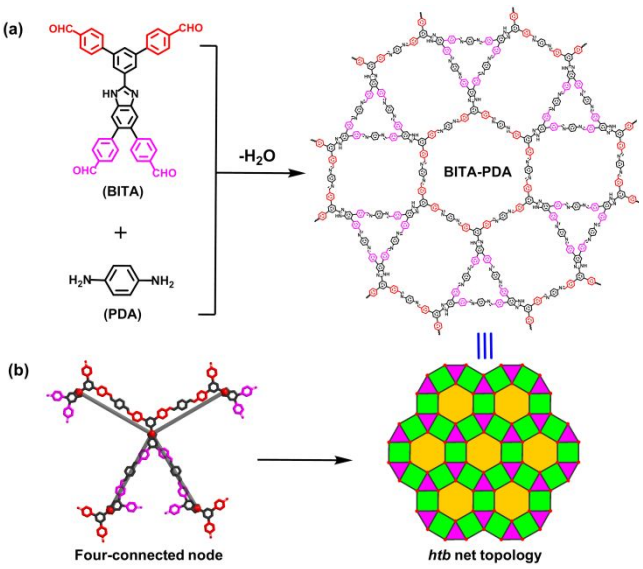


[a] School of Chemistry, South China Normal University, Guangzhou 510006 , P. R. China. E-mail: wgzhang@scnu.edu.cn, zhengsr@scnu.edu.cn
[b] The Molecular Foundry, Lawrence Berkeley National Laboratory, Berkeley, California 94720, United States. E-mail: yliu@lbl.gov

† Electronic Supplementary Information (**ESI**) available: Full synthetic procedure, IR spectra, solid-state $^{13}C$ NMR spectrum, SEM, TGA trace, LC-MS, PXRD analysis and coordinates of crystal structure models. See DOI: 10.1039/b000000x/

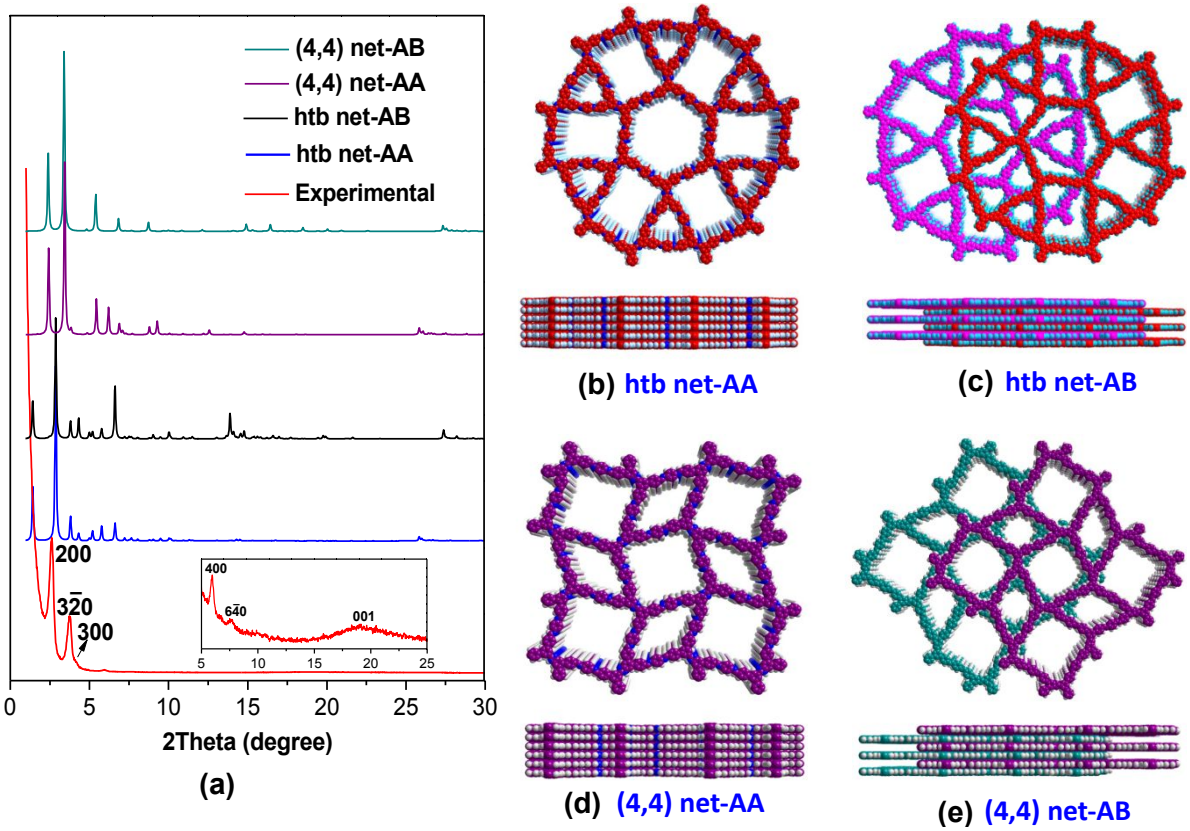


Fig. 1. (a) Experimental PXRD pattern of BITA-PDA COF (red); Simulated PXRD patterns of BITA-PDA COF exhibiting an **htb** or (4,4) net topology**.** Space-filling models of BITA-PDA COF showing an **htb** or (4,4) net topology in (b, d) AA packing mode and (c, e) AB packing mode.

featuring three different kinds of regular polygons (equivalent to a hexagonal tungsten bronze (**htb**) net topology). Optimized condensation reactions of BITA with the diamine PDA resulted in the successful formation of the target BITA-PDA COF with the **htb** topology (Scheme **1**), a hitherto unknown COF topology. The obtained BITA-PDA COF displays selective luminescence response toward $Fe^{3+}$ ion over other metal ions in DMF media, making BITA-PDA COF a potential fluorescent sensor for detection of $Fe^{3+}$ ion.

The synthesis of crystalline BITA-PDA COF was optimized by reacting BITA and PDA with a mole ratio of 1/4 in a degassed mixture of aqueous acetic acid (9 M)/1,2-dichlorobenzene/ethanol (2:13:13 v/v/v) at 110 ˚C for 5 days. Reactions of BITA and PDA under similar conditions but using different molar ratios give rise to the products with very poor or no crystallinity (Fig. S1). Additionally, BITA-PDA COF with fair crystallinity could also be prepared using 1,2-dichlorobenzene/tert-butanol (1:1 v/v) as the solvents (Fig. S2), while the use of other solvents such as dioxane, or mixed dioxane/mesitylene under similar reaction conditions only led to amorphous products.

In order to determine the crystalline structure of the resulting BITA-PDA COF, both powder X-ray diffraction (PXRD) experiments and theoretical simulations were carried out. Two most plausible crystal structures based on a 2D layered **htb** topology, which are the eclipsed AA packing structure with *P*6/*M* space group and the staggered AB packing structure with *P*63/*M* space group, respectively, were constructed by employing Accelrys Materials Studio software and their corresponding simulated PXRD patterns were generated. As presented in Fig. 1a (red curve), BITA-PDA COF exhibits several strong diffraction peaks, indicative of its crystalline nature. The two sharpest and most intense diffraction peaks centered at $2\theta$ = 2.68 and 3.80˚ are ascribed to the (200) and (3$\bar{2}$0) facets, respectively, while the other diffraction peaks at $2\theta$ = 4.26, 5.94, 7.66 and 19.14˚ can be assigned to the (300), (400), (6$\bar{4}$0) and (001) facets, respectively. The experimental pattern is in good agreement with the calculated PXRD patterns (Fig. 1a, blue curve) produced from the simulated structure based on an **htb** type network with AA packing (Fig. 1b). The AA packing model is then utilized for the Pawley refinement by employing Reflex module implemented in Materials Studio software, which shows great agreement with the experimental ones (Fig. S3). The refinement result finally provides a hexagonal unit cell with the optimized parameters of $a = b$ = 72.87 Å, c = 3.24 Å, $\alpha = \beta = 90°$ and $\gamma$ = 120°. Meanwhile, the refinement result yields two good agreement factors with $R_p$ and $R_{wp}$ being 3.17% and 4.48%, respectively. On the contrary, the calculated PXRD pattern (Fig. 1a, black curve) generated from the **htb** type network structure with AB packing (Fig. 1c) does not match well with the experimental PXRD patterns. Two other possible morphologies from the assembly are (4,4) net (Figs. 1d and 1e) and **fwe**-net (Figs. S4d and S4e), which possess two and four different pore sizes. A comparison of the simulated patterns based on their respective AA- and AB-stacking against the experimental data indicated both deviation of the peak at the lowest diffraction angle and inconsistency of the high order peaks. In addition, we have calculated the normalized[33] total formation energy of the three network structures in their AA packing mode. **fwe**-Net has significantly higher formation energy of 333 kcal/mol, while these for (4,4)-net and **htb**-net are comparable (246 kcal/mol vs 252 kcal/mol).

Fourier transform infrared (FT-IR) and solid-state NMR spectroscopy were carried out to confirm the chemical composition of the obtained imine-linked BITA-PDA COF. The FT-IR spectrum of BITA-PDA COF displays an intense peak at 1621 $cm^{-1}$, which is

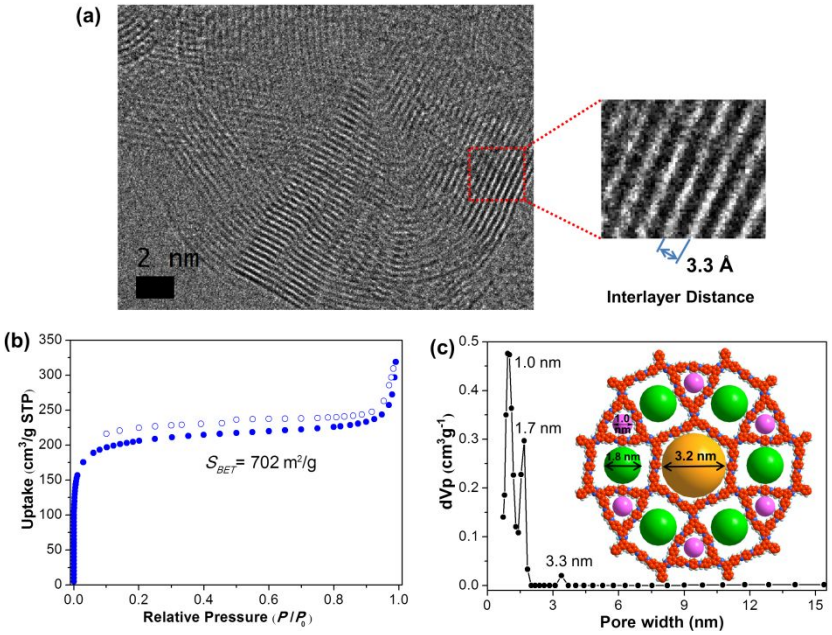


Fig. 2. (a) HRTEM image of the **htb** type BITA-PDA COF showing the interlayer packing structure. (b) $N_2$ adsorption (●) and desorption (○) isotherm curves at 77 K and (c) pore size distribution profile of BITA-PDA COF.

attributable to the characteristic C=N stretching vibrations of imine bonds. Meanwhile, the intensities of aldehyde (1697 $cm^{-1}$) and amino (around 3300 $cm^{-1}$) bands of BITA-PDA COF are decreased in comparison to those of the starting materials BITA and PDA (Figs. S5-S8), consistent with the consumption of these two monomers. The residual band of C=O at around 1697 $cm^{-1}$ can be attributed to the existence of terminal aldehyde groups at the edges of the BITA-PDA COF framework, which is similar to those observed in other 2D COF materials[12,13] The characteristic resonance signals of imine carbons (around 160 ppm) can be found in $^{13}C$ cross-polarization magic-angle spinning (CP-MAS) solid-state NMR spectrum of BITA-PDA COF (Fig. S9), further confirming the existence of the formed imine C=N linkages. The scanning electron microscopy (SEM) image reveals that BITA-PDA COF has a nanoparticle morphology (Fig. S10). Moreover, HRTEM measurement suggests that BITA-PDA COF displays a multilayered structure with the interlayer distance of about 3.3 Å (Fig. 2a), confirming the 2D nature of the formed framework. Additionally, thermogravimetric analysis (TGA) indicates that the as-synthesized BITA-PDA COF is thermally stable under air atmosphere, with only 5.5% weight loss at the temperature of 380 °C (Fig. S11).

Nitrogen adsorption−desorption experiment was conducted at 77 K on the COF samples that were activated by heating at 120 °C for 12 h under a dynamic vacuum. As presented in Fig. 2b, the adsorption curve of BITA-PDA COF exhibits a steep nitrogen uptake in the low relative pressure range ($P/P_0$ = 0−0.01), which is characteristic for porous materials. A surface area of 702 $m^2$ $g^{-1}$ can be calculated when utilizing the Brunauer–Emmett–Teller (BET) model for $P/P_0$ between 0.05 and 0.25 as depicted in Fig. S12, while if the Langmuir model is applied, the resulting surface area is found to be 940 $m^2$ $g^{-1}$ (Fig. S13), all of which are larger than those found for the reported 2D COFs with triple pores.[32,34] Additionally, the total pore volume of BITA-PDA COF is determined to be 0.49 $cm^3$ $g^{-1}$ based on a single point measurement at $P/P_0$ = 0.99. Moreover, the pore size distribution of BITA-PDA COF was produced through a quenched solid density functional theory (QSDFT) to fit the adsorption branch of the nitrogen sorption isotherm. As displayed in Fig. 2c, the BITA-PDA COF exhibits three distributions around 1.0, 1.7, and 3.3 nm, which can be attributed to the trigonal, rectangular, and hexagonal pores, respectively. Such three-pore feature is most consistent with the predicted **htb** net and in contrast to the (4,4) and **fwe** net structures. On the basis of the proposed **htb** type BITA-PDA COF, the three measured diameters are very close to the theoretically calculated trigonal, rectangular and hexagonal pore sizes (1.0, 1.8, 3.2 nm, respectively, Fig. 2c). The above simulations and analyses strongly support the formation of a 2D COF with an **htb** network and AA packing, which, to the best of our knowledge, represents the first example of such type that features three different kinds of pores including trigonal, rectangular, and hexagonal ones.

Previous studies indicated that COF-type materials can be utilized as highly selective fluorescent chemosensors for sensing of metal cations.[14,15] Development of new chemical sensors for recognizing $Fe^{3+}$ ion has attracted much interest because $Fe^{3+}$ ion plays a significant role in life science and biological processes.[32] Thus, we subsequently investigated the sensing abilities of BITA-PDA COF toward various metal cations through fluorescence spectroscopic studies. When dispersing the BITA-PDA powder in DMF solvent, it exhibits blue photoluminescence with a maximum emission band at 432 nm upon excitation at 322 nm (Fig. S14). The metal cation sensing experiments were carried out by the addition of different chloride salts to the BITA-PDA COF suspensions, with the concentration of the metal ion being $1\times10^{-4}$ mol/L. Interestingly, emission spectra of the suspensions indicate that the luminescence intensity of BITA-PDA is mainly dependent on the species of metal ions (Fig. 3a). Addition of metal cations including $Cd^{2+}$, $Sn^{2+}$, $Mg^{2+}$, $Hg^{2+}$, $K^+$, $Li^+$, $Na^+$, $Al^{3+}$, $Sr^{2+}$, $Ni^{2+}$, $Ca^{2+}$, $Cu^{2+}$ and $Co^{2+}$ to the suspensions, respectively, result in almost no or slight change on the fluorescence intensity of BITA-PDA COF, whereas its luminescence intensity is significantly quenched when $Fe^{3+}$ is added (Fig. S15). These results reveal that BITA-PDA COF may be used as a chemical sensor for the detection of $Fe^{3+}$ ion through luminescence quenching. To study the reusability of the luminescent BITA-PDA COF for the detection of $Fe^{3+}$ ions, quenching-recovery experiments were carried out. Repeated experiments were conducted by centrifugation treatment followed by washing the COF material with fresh DMF for several times. As shown in Fig. S16, the emission intensity of the BITA-PDA COF exhibits only ~12% reduction after four quenching-recovery cycles, suggesting the good reusability of the BITA-PDA

COF. For the purpose of better understanding the sensing ability of BITA-PDA towards $Fe^{3+}$ ion, a fluorescence titration experiment that can trace the spectroscopic changes upon the addition of $Fe^{3+}$ to BITA-PDA COF was conduct. As illustrated in Fig. 3b, when the concentration of $Fe^{3+}$ ion is increased from 0 to $1\times10^{-4}$ mol/L, the emission intensity of BITA-PDA COF suspension decreases progressively. A near linear Stern–Volmer plot can be acquired in the low $Fe^{3+}$ concentration range,, giving rise to a quenching constant ($K_{sv}$) value of $2.9\times10^{4}$ L/mol (Fig. S17), which is comparable to those in the MOF-type materials for $Fe^{3+}$ detection.[34,35] Moreover, Fe 2p X-ray photoelectron spectroscopy (XPS) of the $Fe^{3+}$-incorporated BITA-PDA COF (Fig. S18) displays two peaks at 711.6 and 724.9 eV, corresponding to the binding energies of Fe $2p_{3/2}$ and Fe $2p_{1/2}$,[36] respectively, further confirming immobilization of the $Fe^{3+}$ ion into the pore channels of BITA-PDA COF. We postulate that the N atoms from benzimidazole and imine units in the pore walls of BITA-PDA COF are prearranged in a favorable coordination geometry towards $Fe^{3+}$, which are responsible

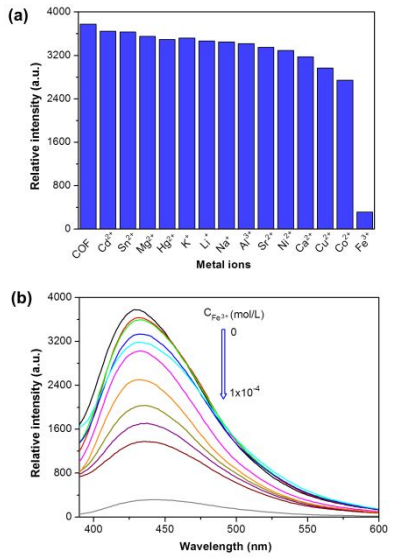


Fig. 3. (a) Comparison of fluorescence intensity of BITA-PDA COF in the presence of various metal ions ($1\times10^{-4}$ mol/L) in DMF ($\lambda_{ex}$ = 322 nm). (b) Emission spectra of BITA-PDA COF in DMF suspensions containing various $C_{Fe3+}$ (0 to $1\times10^{-4}$ mol/L).

for the observed selective luminescence quenching.[15,34]

In summary, we have presented the rational design and targeted construction of a 2D imine-linked BITA-PDA COF with an unprecedented **htb** topology from a linear diamine linker and a tetra-aldehyde building block. Powder X-ray diffraction analysis, HRTEM measurement, together with detailed theoretical simulations and nitrogen adsorption−desorption studies collectively confirmed the formation of the novel 2D **htb** topological network. Moreover, the obtained BITA-PDA COF displays a highly selective and sensitive luminescence response toward $Fe^{3+}$ in DMF, indicating that it may be used as a potential fluorescent sensor for detection of $Fe^{3+}$ ion. This work opens the door to the development of interesting COFs with unprecedented topologies and may broaden the scope of the emerging COF-type functional materials through pore size and pore surface engineering.

We gratefully acknowledge the financial support from the National Natural Science Foundation of P. R. China (Grant Nos. 21603076 and 21571070), the Natural Science Foundation of Guangdong Province (Grant Nos 2016A030310437 and 2018A030313193). Part of the work is carried out as a user project at the Molecular Foundry, which is supported by the Office of Science, Office of Basic Energy Sciences, of the U.S. Department of Energy under Contract No. DE-AC02-05CH11231.

## Notes and references

(1) Y. H. Jin, Y. M. Hu and W. Zhang, *Nat. Rev. Chem.* 2017, 1.
(2) C. S. Diercks and O. M. Yaghi, *Science* 2017, **355**.
(3) N. Huang, P. Wang and D. L. Jiang, *Nat. Rev. Mater.* 2016, **1**.
(4) F. J. Uribe-Romo, J. R. Hunt, H. Furukawa, C. Klock, M. O'Keeffe and O. M. Yaghi, *J. Am. Chem. Soc.*, 2009, **131**, 4570.
(5) H. M. El-Kaderi, J. R. Hunt, J. L. Mendoza-Cortes, A. P. Cote, R. E. Taylor, M. O'Keeffe and O. M. Yaghi, *Science* 2007, **316**, 268.
(6) G. Q. Lin, H. M. Ding, D. Q. Yuan, B. S. Wang and C. Wang, *J. Am. Chem. Soc.*, 2016, **138**, 3302.
(7) O. Yahiaoui, A. N. Fitch, F. Hoffman, M. Froba, A. Thomas and J. Roeser, *J. Am. Chem. Soc.*, 2018, **140**, 5330.
(8) X. Han, Q. C. Xia, J. J. Huang, Y. Liu, C. X. Tan and Y. Cui, *J. Am. Chem. Soc.*, 2017, **139**, 8693.
(9) H. S. Xu, S. Y. Ding, W. K. An, H. Wu and W. Wang, *J. Am. Chem. Soc.*, 2016, **138**, 11489.
(10) S. S. Han, H. Furukawa, O. M. Yaghi and W. A. Goddard, *J. Am. Chem. Soc.*, 2008, **130**, 11580.
(11) Z. H. Xiang,; R. Mercado, J. M. Huck, H. Wang, Z. H. Guo, W. C. Wang, D. P. Cao, M. Haranczyk and B. Smit, *J. Am. Chem. Soc.*, 2015, **137**, 13301.
(12) S. L. Cai, K. Zhang, J. B. Tan, S. Wang, S. R. Zheng, J. Fan, Y. Yu, W. G. Zhang and Y. Liu, *ACS Macro Let.*, 2016, **5**, 1348.
(13) S. Dalapati, S. B. Jin, J. Gao, Y. H. Xu, A. Nagai and D. L. Jiang, *J. Am. Chem. Soc.*, 2013, **135**, 17310.
(14) S. Y. Ding, M. Dong, Y. W. Wang, Y. T. Chen, H. Z. Wang, C. Y. Su and W. Wang, *J. Am. Chem. Soc.*, 2016, **138**, 3031.
(15) G. Chen, H. H. Lan, S. L. Cai, B. Sun, X. L. Li, Z. H. He, S. R. Zheng, J. Fan, Y. Liu and W. G. Zhang, *ACS Appl. Mater. Interfaces*, 2019, **11**, 12830.
(16) H. L. Qian, C. X. Yang and X. P. Yan, *Nat. Commun.*, 2016, **7**.
(17) K. Zhang, S. L. Cai, Y. L. Yan, Z. H. He, H. M. Lin, X. L. Huang, S. R. Zheng, J. Fan and W. G. Zhang, *J. Chromatogr. A*, 2017, **1519**, 100.
(18) X. Hang, J. J. Huang, C. Yuan, Y. Liu and Y. Cui, *J. Am. Chem. Soc.*, 2018, **140**, 892.
(19) J. W. Colson, A. R. Woll, A. Mukherjee, M. P. Levendorf, E. L. Spitler, V. B. Shields, M. G. Spencer, J. Park and W. R. Dichtel, *Science* 2011, **332**, 228.
(20) M. Dogru, M. Handloser, F. Auras, T. Kunz, D. Medina, A. Hartschuh, P. Knochel and T. Bein, *Angew. Chem., Int. Ed.,* 2013, **52**, 2920.
(21) S. L Cai,. Y. B. Zhang, A. B. Pun, B. He, J. H. Yang, F. M. Toma, I. D. Sharp, O. M. Yaghi, J. Fan, S. R. Zheng, W. G. Zhang and Y. Liu, *Chem. Sci.*, 2014, **5**, 4693-4700.
(22) M. O'Keeffe and O. M. Yaghi, *Chem. Rev.* 2012, *112*, 675.
(23) A. P. Cote, A. I. Benin, N. W. Ockwig, M. O'Keeffe, A. J. Matzger and O. M. Yaghi, *Science* 2005, **310**, 1166.
(24) X. S. Ding, J. Guo, X. A. Feng, Y. Honsho, J. D. Guo, S. Seki, P. Maitarad, A. Saeki, S. Nagase and D. L. Jiang, *Angew. Chem., Int. Ed.,* 2011, **50**, 1289.
(25) S. Dalapati, M. Addicoat, S. B. Jin, T. Sakurai, J. Gao, H. Xu, S. Irle, S. Seki and D. L. Jiang, *Nat. Commun.*, 2015, **6**.
(26) T. Y. Zhou, S. Q. Xu, Q. Wen, Z. F. Pang and X. Zhao, *J. Am. Chem. Soc.*, 2014, **136**, 15885.
(27) S. Q. Xu, R. R. Liang, T. G. Zhan, Q. Y. Qi and X. Zhao, *Chem. Commun.*, 2017, **53**, 2431.
(28) B. Zhang, H. Y. Mao, R. Matheu, J. A. Reimer, S. A. Alshmimri, S. Alshihri and O. M. Yaghi, *J. Am. Chem. Soc.*, 2019, **141**, 11420.
(29) Y. L. Zhu, S. Wan, Y. H. Jin and W. Zhang, *J. Am. Chem. Soc.*, 2015, **137**, 13772.
(30) N. Huang, L. P. Zhai, D. E. Coupry, M. A. Addicoat, K. Okushita, K. Nishimura, T. Heine and D. L. Jiang, *Nat. Commun.*, 2016, **7**.
(31) C. Qian, S. Q. Xu, G. F. Jiang, T. G. Zhan and X. Zhao, *Chem-Eur. J.*, 2016, **22**, 17784.
(32) Z. F. Pang, S. Q. Xu, T. Y. Zhou, R. R. Liang, T. G. Zhan and X. Zhao, *J. Am. Chem. Soc.*, 2016, **138**, 4710.
(33) C. Qian, Q. Y. Qi, G. F. Jiang, F. Z. Cui, Y. Tian and X. Zhao, *J. Am. Chem. Soc.*, 2017, **139**, 6736.
(34) Z. C. Hu, B. J. Deibert and J. Li, *Chem. Soc. Rev.* 2014, **43**, 5815.
(35) C. Q. Zhang, Y. Yan, Q. H. Pan, L. B. Sun, H. M. He, Y. L. Liu, Z. Q. Liang and J. Y. Li, *Dalton Trans.*, 2015, **44**, 13340.
(36) Z. H. Xu and J. G. Yu, *Nanoscale* 2011, **3**, 3138.

TOC graphic for

# An unprecedented 2D covalent organic framework with an htb net topology †

Song-Liang Cai,[a,b] Zi-Hao He,[a] Xin-Le Li,[b] Kai Zhang,[a] Sheng-Run Zheng,*[a] Jun Fan,[a] Yi Liu*[b] and Wei-Guang Zhang*[a]

An imine-based two-dimensional covalent organic framework with an unprecedented **htb** type topology has been rationally designed and successfully synthesized for the first time.